The structure of the Winds of η Car as seen by HST/STIS and VLTI/AMBER

K. E. Nielsen (CUA & NASA/GSFC), G. Weigelt (MPIfR), T. R. Gull (NASA/GSFC), M. F. Corcoran (USRA & NASA/GSFC), T. Driebe (MPIfR), S. Kraus (MPIfR), K. Hamaguchi (USRA & NASA/GSFC) & D. J. Hillier (U. Pittsburgh)

nielsen@milkyway.gsfc.nasa.gov

Introduction

Eta Carinae (η Car) has fascinated astronomers since its major event in the 1840s, when it rivaled Sirius in apparent magnitude for nearly two decades, then faded, only to brighten again in the 1890s. Today we see the central source with 6×10^6 $L_\odot$ and a wind of 10^{-3} $M_\odot$/yr at 600 km s^{-1}. A massive binary lies within an extended wind in turn engulfed by its ejecta, the Homunculus (1840s event) and the Little Homunculus (1890s). Damineli (1996) found a spectroscopic 5.5-year periodicity in He I λ10830. The minimum coincides with a drop in X-rays which also recurs with a 5.54 year period (Corcoran 2005).

We present temporal surface plots of selected He I, H I and Fe II stellar line profiles measured with *HST*/STIS sampled from 1998.0 to 2004.3. Our spectra show variations in line profiles that can be attributed to radial velocity variations of the primary star and ionization effects due to the hot companion combined with its wind cavity. We also present the first near infrared spectro-interferometry of η Car (Weigelt et al. 2006). These observations were performed with ESO/VLTI AMBER instrument in 2004.9 and 2005.1.

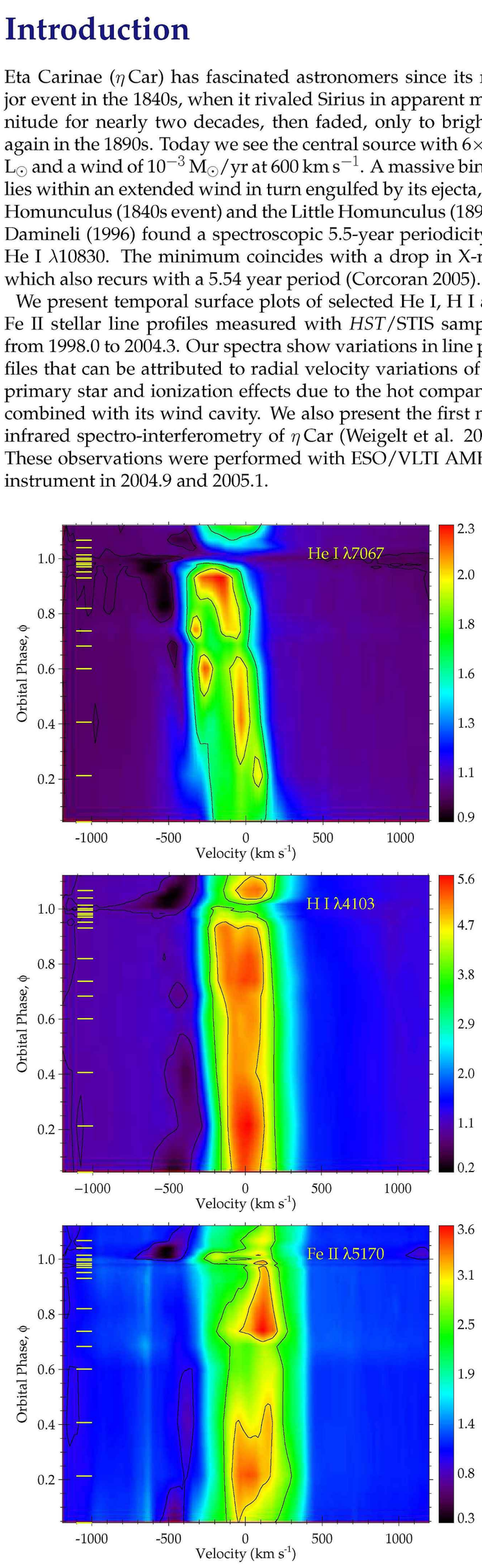

Figure 1: **Temporal surface plots of stellar line profiles from 1998.0 (ϕ =0.0) to 2004.3 (ϕ =1.2). From the top: He I λ7067, H I λ4103 (Hδ) and Fe II λ5170.**

Analysis

We examined the changes in stellar wind line profiles for multiple lines sampling a range of ionization potentials: He I (24.6 − 54.4 eV), H I (13.6 eV) and Fe II (7.9 − 16.2 eV). Changes in emission and absorption line profiles are apparent during the two observed spectroscopic minima (1998.0, ϕ =0 and 2003.5, ϕ =1.0). In Figure 1 we show the time variability of the line profiles and absorption velocity shifts across the observational interval. This variability is caused by the interaction with the companion star (η Car B). The blue-shifted He I profile places η Car B at apastron on the observer's side of the primary. The hotter, faster and less massive η Car B wind is blowing a cavity out of the primary wind. The companion's UV radiation ionizes an adjacent portion of the primary wind to He^+ which shifts in shape and position as η Car sweeps around its orbit.

We created a simple model of the He^+ zone (Figure 2) to understand the source of the He I emission and absorption. Models of η Car (Hillier et al. 2005) show that little He I emission is due to the primary star exciting its own stellar wind. Helium is mainly neutral in the primary wind as far UV photons are required to even populate the lowest excited states. The He I lines represent the highly excited regions of the bow-shock and the adjacent portion of the primary wind. The blue-shifted, narrow emission line components originate from the cooling region beyond the wind-wind interface extending into the primary wind to the boundary of the hard UV radiation of the hot companion. Absorption originates from the He^+ region of the primary wind in line-of-sight from the primary star to the observer.

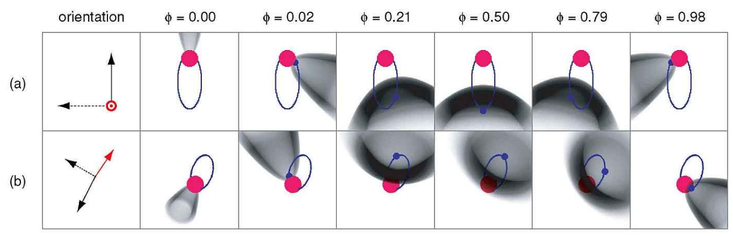

Figure 2: **Visualization of the He^+ zone located in the η Car system. Top row (a) views the system with the plane lying in the sky: the Z-axis (red) points into the paper, the X-axis (dashed arrow) and the Y-axis (solid) lie in the skyplane. The orbital major axis is in the -Y direction and the minor axis in the -X direction. Bottom row (b) views the system with the Z-axis (red) pointed along the axis of the bipolar Homunculus (−41° into the plane). NOTE: The model does not include the coriolis distortions which dominate near periastron, but are small near apastron (ϕ =0.5).**

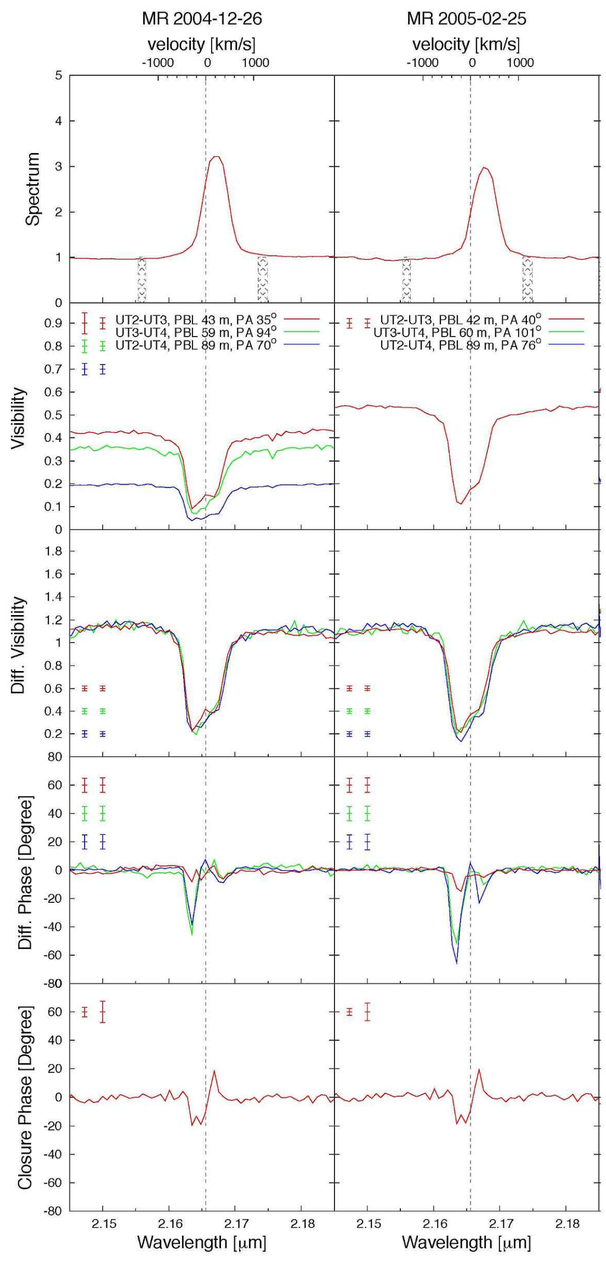

Figure 3: **AMBER observables from the η Car data around H I Brγ (Left: MR 2004 December 26, Right: MR, 2005 February 25). The first row shows the continuum-normailized spectra as extracted from the interferometric channels, follow by the derived calibrated visiblilities and the differential visibilities. In the forth and fifth row, the differential phase and the closure phase are presented. The vertical grey line marks the rest-wavelength of H I Brγ (λ2.17 μm). The left error bars correspond to the total error for the wavelength range within the line.**

The spectrally dispersed interferograms from VLTI/AMBER (Figures 3 & 4) allow investigations of the wavelength dependence of the visibility, differential phase, and closure phase. The AMBER measurements are in good agreement with predictions of the radiative transfer model of Hillier et al. (2001). If a Hillier et al. (2001) model visibilities are fitted to the observed AMBER visibilities, we obtain 50% encircled-energy diameters of 4.3, 6.5 and 9.6 mas in the 2.17 μm continuum, the He I, and the He I Brγ emission lines, respectively. These observations support theoretical models of anisotropic winds from fast-rotating, luminous hot stars with enhanced high-velocity mass loss near the polar regions.

Discussion

The He I absorption samples a subset of the interacting winds and the H I absorption has a very significant time delay that damps the orbital variations. However, these observations suggest that the secondary star and its wind cavity sample the primary wind to considerable depth during periastron. A detailed hydrodynamic model is required to interpret the radial velocity measures in order to obtain a mass function. With such a model in hand, we will learn much about wind properties, including clumping and ionization structure, by future selective observations especially across periastron in Jan 2009.

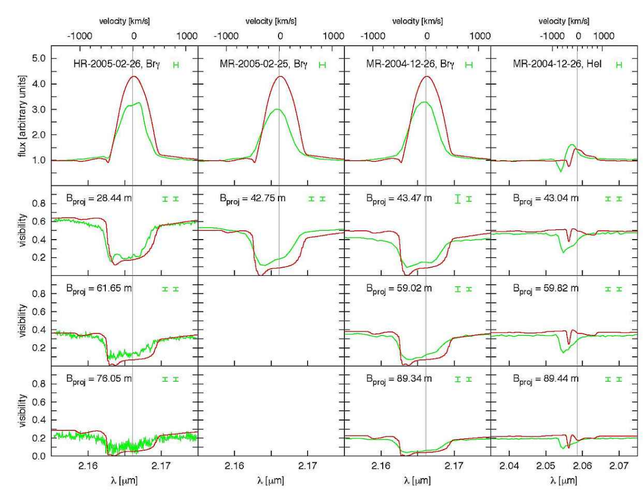

Figure 4: **Comparison of the AMBER spectra and visibility with the NLTE model predictions of Hillier et al. (2001). The figure displays the spectra (upper row) and visibilities (lower three rows) of the four AMBER measurements (green lines) and the corresponding data of the Hillier et al. NLTE model (red lines). Note that no additional scaling has been applied to the Hillier et al. model.**

The AMBER visibilities are in good agreement with the radiative transfer model predictions from Hillier et al. (2001) as shown in Figure 4. In the K-band continuum, we found an elongation toward position angle 128±15° with a projected axis ratio of 1.21±0.08 (2-D visibility fit). This result confirms the earlier finding of van Boeckel et al. (2003) and supports theoretical studies which predict an enhanced mass loss in polar direction for massive stars rotating close to their critical rotation rate (e.g. Dwarkadas & Owocki 2002). We developed a physically motivated model which shows that the asymmetries measured within the line wings are consistent with the geometry expected for an aspherical, latitude-dependent stellar wind (Weigelt et al. 2006).

This work is based upon STIS GTO and HST GO, η Car Treasury observations made with the NASA/ESA HST, obtained at the STScI, which is operated by AURA under NASA contract NAS 5 – 26555. Intermediate CCD data reduction products were obtained from http://etacar.umn.edu.